Am J Physiol Lung Cell Mol Physiol 289: L497–L508, 2005.
First published May 13, 2005; doi:10.1152/ajplung.00100.2005.

Differences in the translation efficiency and mRNA stability mediated by 5′-UTR splice variants of human SP-A1 and SP-A2 genes

Guirong Wang,[1]* Xiaoxuan Guo,[1]* and Joanna Floros[1,2,3]

Departments of [1]Cellular and Molecular Physiology, [2]Pediatrics, and [3]Obstetrics and Gynecology, The Pennsylvania State University College of Medicine, Hershey, Pennsylvania

Submitted 4 March 2005; accepted in final form 5 May 2005

Wang, Guirong, Xiaoxuan Guo, and Joanna Floros. Differences in the translation efficiency and mRNA stability mediated by 5′-UTR splice variants of human SP-A1 and SP-A2 genes. *Am J Physiol Lung Cell Mol Physiol* 289: L497–L508, 2005. First published May 13, 2005; doi:10.1152/ajplung.00100.2005.—Surfactant protein A (SP-A) plays an important role in host defense, modulation of inflammatory processes, and surfactant-related functions of the lung. The human SP-A (hSP-A) locus consists of two functional genes, *SP-A1* and *SP-A2*. Several hSP-A 5′-untranslated region (UTR) splice variants for each gene have been characterized and shown to be translated in vitro and in vivo. In this report, we investigated the role of hSP-A 5′-UTR splice variants on SP-A production and molecular mechanisms involved. We used in vitro transient expression of hSP-A 5′-UTR constructs containing luciferase as the reporter gene and quantitative real-time PCR to study hSP-A 5′-UTR-mediated gene expression. We found that *1*) the four (A′D′, ABD, AB′D′, and A′CD′) 5′-UTR splice variants under study enhanced gene expression, by increasing luciferase activity from 2.5- to 19.5-fold and luciferase mRNA from 4.3- to 8.8-fold compared with the control vector that lacked hSP-A 5′-UTR; *2*) all four 5′-UTR splice variants studied regulated mRNA stability. The ABD variant exhibited the lowest rate of mRNA decay compared with the other three constructs (A′D′, AB′D′, and A′CD′). These three constructs also exhibited significantly lower rate of mRNA decay compared with the control vector; *3*) based on the indexes of translational efficiency (luciferase activity/mRNA), ABD and AB′D′ exhibited higher translational efficiency compared with the control vector, whereas the translational efficiency of each A′D′ and A′CD′ was lower than that of the control vector. These findings indicate that the hSP-A 5′-UTR splice variants play an important role in both SP-A translation and mRNA stability.

surfactant protein A; 5'-untranslated region; regulation; NCI-H441 cell line; translational control

SURFACTANT PROTEIN A (SP-A), the most abundant surfactant-associated protein in the alveolar lung space (12), plays an important role in host defense, the modulation of inflammatory processes, as well as in surfactant physiology including surfactant structure and metabolism (8, 13, 50, 57). SP-A is an extensively modified sialoglycoprotein with molecular mass ~30–35 kDa under reduced conditions (20, 60). Under native conditions three SP-A molecules form a trimer and six trimers form a "flower-like" structure through oligomerization of the NH_2-terminal and collagen-like domains (69). In humans SP-A is expressed in alveolar epithelial type II cells (59), Clara cells (49), in tracheal and bronchial submucosal gland cells, as well as tissues other than lung (18, 45, 48, 49, 63). In animal species SP-A is also expressed in the bronchiolar epithelium of the lung (58).

The human SP-A (hSP-A) locus consists of two functional genes, SP-A1 and SP-A2, and a pseudogene (26). Genomic sequences for both SP-A1 and SP-A2 genes (38, 76) and their corresponding cDNAs (15) have been published. Several alleles for each hSP-A gene have been characterized based on the DNA sequence variation at the coding region (10, 11). Structural and functional differences between SP-A1 and SP-A2, as well as among some frequently observed alleles, have been observed (17, 65, 71, 73, 74).

The genomic structure of SP-A1 and SP-A2 consists of a 5′-untranslated region (UTR), four coding exons, and a 3′-UTR, which is part of the fourth coding exon (38, 76). The 5′-UTR of the SP-A genes is complex. Four exons or regions (A, B, C, D) for SP-A1 or three (A, B, D) for SP-A2 (36), shown in Fig. 1, splice in a number of configurations to form different 5′-UTR. The major splice patterns, as well as their relative frequency, vary between the two genes; the major pattern for SP-A1 is A*D′ (81%), and the major patterns for SP-A2 are A*BD (44%) and A*BD′ (49%) based on our previous observation (36), where no distinction was made among the three transcription start sites of exon A (36). All three start sites (A, A′, A″) were denoted here as exon A*. The major 5′-UTR splice variants of the mRNA transcripts of each SP-A gene are shown to be translated both in vitro (36) and in vivo (37).

SP-A expression is regulated at several levels, including at the tissue-specific level, by development stage, by a number of hormones, and other factors (52). Studies of hSP-A regulation by glucocorticoids (GC) in fetal lung explants (5, 32, 34, 43), of the 5′-flanking region (29), and of the 3′-UTR (27, 72) of SP-A have produced a complex picture of regulation. In fact, the two SP-A genes have been shown to be differentially regulated by certain agents including GC (29, 34, 43, 51, 64), and certain SP-A alleles may be differentially regulated by dexamethasone (Dex, a synthetic GC) (27, 72). Previous reports of the promoter of SP-A1 revealed that the −32/+63 region relative to the SP-A1 transcription start site was sufficient for both basal transcription and Dex repression (29). Removal of the +18/+63 region significantly reduced the ability of Dex to inhibit transcription. *Cis*-elements similar to negative GR-binding sites were identified within the −32/+63 region (29).

Recent studies have shown that 5′-UTR plays an important role in the regulation of gene expression (see reviews, Refs. 19,

* G. Wang and X. Guo contributed equally to this work.

Address for reprint requests and other correspondence: J. Floros, Dept. of Cellular and Molecular Physiology, H166, Penn. State Univ. College of Medicine, 500 Univ. Dr., Hershey, PA 17033 (e-mail: jfloros@psu.edu).

The costs of publication of this article were defrayed in part by the payment of page charges. The article must therefore be hereby marked "*advertisement*" in accordance with 18 U.S.C. Section 1734 solely to indicate this fact.

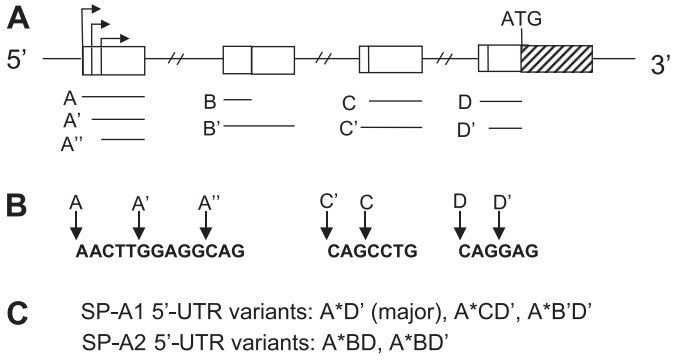

Fig. 1. Diagram of human surfactant protein A (hSP-A) 5′-untranslated region (UTR) exons (*A*), 5′-end exon sequence (*B*), and 5′-UTR SP-A1 and SP-A2 splice variants (*C*) (36). *A*: the 4 SP-A untranslated exons designated A, B, C, D (not drawn to scale). Exons A, C, and D vary in length at their 5′-ends and exon B at its 3′-end; the length variation is shown by the solid line below each exon. The SP-A1 gene has been identified with 3 (A, A′, A″) transcription start sites. The size of exons A, A′, and A″ is 44, 39, and 34 nt, respectively; exons B and B′ are 30 and 70 nt, respectively; exons C and C′ are 60 and 63 nt, respectively; exons D and D′ are 26 and 23 nt, respectively. The SP-A2 start site is that of A plus 1 nt upstream. *B*: the 3 transcription start sites for exon A and the 5′-end sequence differences of exons C and D. *C*: the 5′-UTR splice variants of SP-A1 and SP-A2 as characterized previously (36), where no distinction was made among the 3 transcription start sites of exon A. All 3 start sites (A, A′, A″) are denoted here as exon A*, in the SP-A1 and SP-A2 splice variants shown.

56, 68) in a variety of organisms (microbes, plants, animals). The 5′-UTR-mediated regulation has been shown to modulate gene expression both through stimulatory (3, 4, 7, 21, 66) and inhibitory mechanisms (25, 41). These include mechanisms that influence RNA transcription (2, 30, 75), posttranscriptional modification of RNA (secondary structure and mRNA stability) (6, 9, 21, 30, 39), and alteration of translational efficiency (4, 25, 61, 77). For the latter a recent study found that 5′-UTR splice variants of the insulin-like growth factor I (16), insulin (66), and the estrogen receptor-α (41) had different translational efficiencies.

Although several 5′-UTR transcripts of SP-A1 and SP-A2 have been identified and characterized, and it has been shown that these 5′-UTR splice variants can be translated both in vitro (36) and in vivo (37), the regulatory mechanisms involved are not well understood. In this study, we investigated the differential impact of hSP-A 5′-UTR variants on SP-A gene expression by studying translation efficiency, mRNA content, and mRNA stability. Toward this goal we used in vitro transient transfections of several 5′-UTR constructs in the human NCI-H441 (H441) cells (these cells express SP-A). The observations made indicate that the hSP-A 5′-UTR splice variants may contribute to the complexity of SP-A gene expression.

MATERIALS AND METHODS

Cell culture. The human lung adenocarcinoma cell line (H441) used in this study was purchased from the American Type Culture Collection (Manassas, VA). H441 cells were grown in RPMI-1640 medium (Invitrogen Life Technologies, Carlsbad, CA) with 10% heat-inactivated fetal bovine serum (FBS; Summit Biotechnology, Ft. Collins, CO), 1× antimycotic-antibiotic solution (Sigma, St. Louis, MO), and 1% L-glutamine (Sigma). The cells were subcultured weekly and maintained at 37°C in 5% CO_2 atmosphere.

Plasmid constructs. The pcDNA3 vector was purchased from Invitrogen and was modified to facilitate cloning of the 5′-UTRs of human SP-A variants in front of a luciferase reporter gene using PCR cloning with the appropriate primers. First, the pcDNA3 vector was modified by removing one putative transcription start site in pcDNA3. Briefly, the pcDNA3 was digested with *Bam*HI and *Eco*RI restriction enzymes to remove a 33-bp fragment of pcDNA3. The large fragment (~5.3 kb) of pcDNA3 was purified using the QIAquick PCR purification kit (Qiagen, Valencia, CA). Then PCR was performed with primer pair 1046/1047 (Table 1) using the large purified fragment of pcDNA3 as template. Primer 1046 contains *Hin*dIII and *Bam*HI restriction sites in its 5′-ends, and primer 1047 contains *Xho*I and *Bam*HI restriction sites in its 5′-ends. The PCR conditions consisted of 1× *buffer 2*, 0.125 mM of each dNTP, 1 ng/μl of each of the primers, and 3.5 units of Expand high-fidelity PCR system (Roche, Mannheim, Germany) in 50 μl of final volume. The cycling was at 94°C for 2 min, followed by 20 cycles at 94°C for 10 s, 65°C for 30 s, and 68°C for 7 min. The final extension step was at 68°C for 10 min. The PCR products were purified and digested with the *Bam*HI restriction enzyme and then ligated with the T_4 DNA ligase at 4°C overnight. These modifications removed a 133-bp from nucleotide 836 to 970 of pcDNA3, leaving only one *Bam*HI restriction enzyme site in the vector. Transformation in *Escherichia coli* strain XL1 Blue was performed by standard protocol. Purification of plasmid was performed with QIAprep spin miniprep kit (Qiagen). The sequence of the modified pcDNA3 (rpcDNA3) vector was verified by DNA sequencing (Molecular Genetics Core Facility at Pennsylvania State University College of Medicine).

Second, the firefly luciferase gene was cloned into rpcDNA3 vector. The 1.7 kb of firefly luciferase gene fragment was generated by digestion of the pGEM-luc DNA (Promega, Madison, WI) with restriction enzymes *Xho*I/*Bam*HI. This 1.7-kb fragment was then cloned into *Xho*I/*Bam*HI-digested rpcDNA3 vector (Fig. 2). The recombinant plasmid DNA (rpcDNA3/LUC) was confirmed by sequencing.

Third, the hSP-A 5′-UTR variants were each inserted between the promoter and the luciferase reporter gene of the vector (rpcDNA3/LUC) to generate the recombinant constructs under study. SP-A cDNA clones, each containing a different variant transcript of hSP-A, were used as templates to obtain the 5′-UTR variant sequence for cloning. PCR was performed with primer pair 1050/1502 or 1051/1052 (Table 1). Primer 1050 or 1051 contained a *Hin*dIII restriction site at its 5′-end, and 1052 contained a *Bam*HI restriction site at its 5′-end. Primer 1050 was for exon A of 5′-UTR, and 1051 was for exon A′ of 5′-UTR. Primer 1052 was for both D and D′ regions of 5′-UTR. The PCR conditions consisted of 1× *buffer 2*, 0.125 mM of each dNTP, 1 ng/μl of each of the primers, and 7 units of Expand high-fidelity PCR system (Roche) in 100 μl of final volume. PCR was performed at 94°C for 2 min, followed by 25 cycles at 94°C for 30 s, 55°C for 1 min, and 72°C for 1 min. The final extension step was at 72°C for 5 min. The PCR product was purified by electrophoresis with 1.5% BioGel of the MERmaid spin kit (Bio101, La Jolla, CA). The pure PCR products were digested with *Hin*dIII/*Bam*HI and then were cloned into the *Hin*dIII/*Bam*HI site of rpcDNA3/LUC.

Fourth, because the cytomegalovirus (CMV) promoter is a very strong promoter, we speculated that it may not be appropriate for our study. With a strong promoter, we may run the risk of cofactor limiting reaction. Therefore, we replaced the CMV promoter of rpcDNA3/5′-UTR/LUC construct with the SV40 promoter. The SV40 promoter DNA fragment was generated from the pSVLSV40CAT by PCR amplification with primer pair 1082/1083. Primer 1082 contains an *Nru*I restriction site in its 5′-end and 1083, an *Hin*dIII restriction site, at its 5′-end. Primer 1082 sequence starts at nucleotide 4831 and ends at 4849 of pSVL SV40 late promoter expression vector (Pharmacia Biotech, Piscataway, NJ). Primer 1083 starts at nucleotide 328 and ends at 308 of pSVL SV40 late promoter expression vector (Table 1). The PCR reaction was performed in 1× *buffer 2*, 0.0625 mM of each dNTP, 1 ng/μl of each of the primers, and 3.5 units of Expand high-fidelity PCR system (Roche) in 50 μl of final volume under the

Table 1. *Primers used in this study*

Primer Name	Sequence, 5′ to 3′	Comments	Position, bp
1046	CCCggatccACTaagcttCTCTAGTTAGCCAGAGAG	Vector pcDNA3 remodeling, antisense	836~817
1047	GGGggatccCTCGAGCATGCATCTAGAGG	Vector pcDNA3 remodeling, sense	973~990
1050	GGGaagcttAACTTGGAGGCAGAGACC	Human SP-A specific, sense	+1~+18
1051	GGGaagcttGGAGGCAGAGACCCAAGC	Human SP-A specific, sense	+6~+24
1052	CCCggatccGGCTCTGGGTCCAGTCGC	Human SP-A specific, antisense	+921~+904
1082	GGCtcgcgaTTGCAAAAGCCTAGGCCTC	Vector pSVL for SV40 promoter, sense	4830~4849
1083	GGCaagcttAAATAACCTCTGAAAGAGGAA	Vector pSVL for SV40 promoter, antisense	328~308
1152	GCCCGCGAACGACATTTA	Forward primer for pGL3	
1153	TTTGCAACCCCTTTTTGGAA	Reverse primer for pGL3	
1156	GCAGCATATCTTGAACCATTCAAA	Forward primer for pRL-SV40	
1157	CATCACTTGCACGTAGATAAGCATTATA	Reverse primer for pRL-SV40	
Probe-pGL	6-FAM-CATTTCGCAGCCTACCGTGGTGTTC-TAMRA	Probe for pGL3	
Probe-pRL	VIC-TATCATGGCCTCGTGAAATCCCGTTAGTAA-TAMRA	Probe for pR1-SV40	

Nucleotide positions are relative to transcriptional start site (+1) of human surfactant protein (SP)-A except for primers 1046, 1047, 1082, 1083, and 1053. The latter are for the indicated vector sequences. Lower case indicates the additional sequences present in the given primers. These sequences are restriction enzyme recognition sites (see MATERIALS AND METHODS).

following conditions: 94°C for 2 min, and 30 cycles at 94°C for 30 s, 60°C for 30 s, and 72°C for 1 min. The final extension step was at 72°C for 5 min. The PCR product was digested with *Nru*I/*Hin*dIII and cloned into rpcDNA3/5′-UTR/LUC, and in rpcDNA/LUC control vector (not shown), to generate recombinant constructs that contained the SV40 promoter SP-A 5′-UTR and the firefly luciferase gene (Fig. 2). The construct sequences were verified by DNA sequencing. To obtain plasmid DNA for transfection experiments, a large-scale purification of plasmids was performed using the Qiagen plasmid maxi kit. Plasmid DNA was subsequently extracted with phenol-chloroform to eliminate protein contamination.

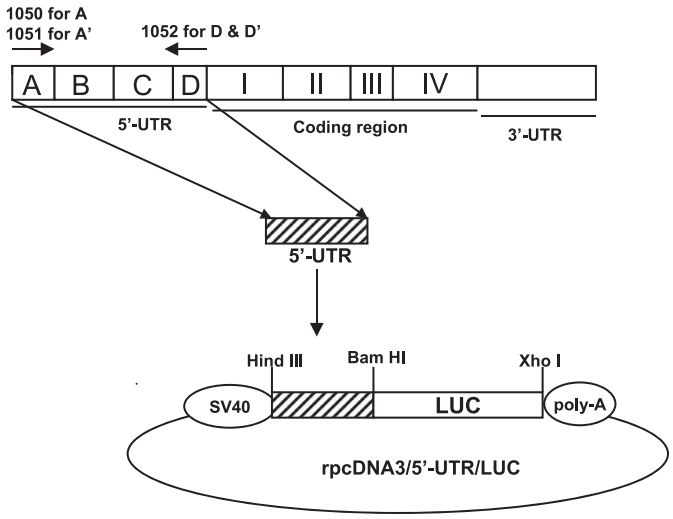

Fig. 2. Schematic representation of recombinant constructs of rpcDNA3/5′-UTR/LUC. The pcDNA3 vector was modified by introducing 2 restriction enzyme sites *Bam*HI and *Xho*I in its multiple cloning site. A fragment of ~1.7 kb of the firefly luciferase gene was amplified from the pGEM-luc vector and cloned into the *Bam*HI/*Xho*I site of the above modified pcDNA3 vector. The cytomegalovirus promoter of the modified pcDNA3 was replaced by the SV40 promoter as described in the MATERIALS AND METHODS. hSP-A 5′-UTR sequences varying from 62 to 137 bp were obtained from hSP-A cDNA clones and cloned into the *Hin*dIII/*Bam*HI restriction enzyme sites of the modified vector. Thus the final recombinant construct (rpcDNA3/5′-UTR/LUC) contained the marker firefly luciferase gene and an hSP-A 5′-UTR splice variant located between the SV40 promoter and the firefly luciferase reporter gene. Four such constructs were generated, each containing a different 5′-UTR variant. The construct without hSP-A 5′-UTR fragment was used as an SP-A control and was referred to as LUC.

Transient transfection and luciferase activity assay. H441 cells were grown to 80–90% confluence in 10-cm dishes and subcultured into six-well culture plates with 1×10^6 cells/well (~80% confluence) 24 h before transfection. Four hours before transfection, the RPMI-1640 plus 10% FBS was replaced with Dulbecco's modified Eagle's medium (DMEM, Invitrogen) containing neither FBS nor antibiotics.

The transfection procedure was performed with the Lipofectamine Plus reagent kit (Invitrogen). In brief, 1 μg of DNA experimental construct plus 0.05 μg of DNA of the transfection efficiency control pRL-SV40 plasmid (containing *Renilla* luciferase as the reporter gene) were diluted in 100 μl of DMEM without serum. PLUS reagent (6 μl) was added, and the mixture was incubated for 15 min at room temperature. In another tube, 4 μl of Lipofectamine reagent were diluted into 100 μl of DMEM without serum. Then, the components of the two tubes were combined, mixed, and incubated for another 15 min at room temperature. The above DNA-Lipofectamine complex was added to each well containing ~1×10^6 H441 cells with 2.5 ml of fresh medium. Four hours after transfection, the DMEM with 10% FBS was added to normal culture volume (5 ml/well). Transfection was carried out for 36 h or for the indicated time for the time course of gene expression.

The dual-luciferase assay was performed with the Dual-luciferase reporter assay system (kit) (Promega). Transfected cells were harvested at 36 h after transfection or at other time points according to statements in the individual experiments. The cells were washed with 1× PBS and were dissolved in 500 μl of 1× passive lysis buffer. The culture plates were rocked at room temperature for 15 min, and the lysate was transferred to a tube and centrifuged for 1 min at 4°C to clear the cell lysate. Twenty microliters of cell extract were transferred into a luminometer tube containing 100 μl of luciferase assay reagent II. The tube was placed in the FB12 luminometer (Zylux, Maryville, TN) and Stop & Glo Reagent (100 μl) was placed into the tube to initiate the *Renilla* luciferase activity reading. The ratio of firefly luciferase activity to *Renilla* luciferase activity was calculated. In all the experiments, transfection and luciferase assays were performed in triplicate.

Total mRNA preparation and measurement by quantitative real-time PCR. Total mRNA was prepared from cells according to instructions of the RNA-Bee kit (TEL-TEST, Friendswood, TX). In brief, the culture medium in the wells was removed, and the cells were washed with PBS buffer. One milliliter of RNA-Bee solution was added, and the cells were homogenized after addition of 0.2 ml of chloroform. After centrifugation at 12,000 *g* for 10 min at 4°C, the aqueous phase was transferred to a clean tube, and total RNA was precipitated by adding 0.5 ml of isopropanol for 5–10 min at room temperature and

centrifuged at 12,000 *g* for 5 min at 4°C. The pellet was washed with 75% ethanol and dissolved in RNase-free double-distilled H_2O. Any contaminating DNA was removed from the RNA preparations using a "DNA-free" kit (Ambion, Austin, TX).

Quantitative real-time PCR was performed using the ABI PRISM 7700 sequence Detection system and a kit of TaqMan one-step RT-PCR Master Mix Reagents (Applied Biosystems, Foster City, CA). In the present study, the real-time PCR probes and primers were designed to target the luciferase gene. With this design the influence of the endogenous SP-A gene expression of the host cells (H441) on the mRNA levels measured is eliminated. No luciferase gene activity was detected in the host cells. In brief, 100 ng of RNA were added into 50 μl of real-time-PCR mix buffer. The buffer contained a forward-reverse primer pair (each 50 nM), such as that of primer pair 1152/1153, and a probe, such as the probe-pGL (see Table 1), as well as other enzymes and reagents provided by the manufacturer (Applied Biosystems). The reaction was carried out via two steps *1*) one cycle at 48°C for 30 min and 95°C for 10 min was performed to reverse transcribe the luciferase mRNA from each RNA preparation to cDNA, and *2*) a real-time PCR reaction was carried out under the following conditions, 43 cycles, each at 95°C for 15 s and 60°C for 1 min. Then the threshold cycle or the number of cycles, where accumulation of PCR products can be detected, was determined (this occurs when fluorescence passes the baseline or fixed threshold). The threshold cycle number was used to determine the number of copies of the standard curve of the control plasmid (see below). The copy number of reporter luciferase cDNA in 100 ng of total RNA was determined and was used as a measurement for the mRNA content. To determine the copy number of the reporter luciferase cDNA, the control plasmid DNA (LUC) was used as standard. The concentrations of the control plasmid DNA varied from 10^{-6} to 1 μg in a 50-μl real-time PCR reaction. The copy number of the plasmid at each concentration and for different numbers of real-time PCR cycles was calculated with the following formula: i.e., copy number per gram of plasmid DNA is equivalent to (6.02×10^{23})/(bp number of plasmid × 660 Da/bp). According to the formula, 1 μg of 7-kb plasmid DNA has 1.3×10^{11} copies of plasmid molecules. Then the standard curve of the control plasmid DNA (number of copies vs. number of real-time PCR cycles) was used to calculate the number of copies in each experimental sample per 100 ng of total RNA in this study. To compare mRNA content of SP-A 5′-UTR variants at 30-h time point after transfection, the relative mRNA level of each SP-A 5′-UTR variants was calculated by normalizing each SP-A 5′-UTR variants to LUC control.

Prediction of RNA secondary structure. To study differences in mRNA secondary structure among hSP-A 5′-UTR variants, the sequences of SP-A 5′-UTR variants were analyzed with an online program (version 3.1) prepared by Dr. M. Zuker (78–80) (http://www.bioinfo.rpi.edu/applications/mfold/old/rna/). Through this type of analysis we were able to predict the secondary structure of hSP-A 5′-UTR variants.

Analysis of mRNA stability following inhibition of transcription by actinomycin D. Actinomycin D, a polypeptide-containing antibiotic, can inhibit transcription through binding tightly and specifically to double-helical DNA. Actinomycin D has been extensively used as a highly specific inhibitor of the formation of new RNA in both prokaryotic and eukaryotic cells (21, 70). In this experiment, H441 cells were transiently transfected with plasmid DNA containing the SP-A 5′-UTR and the reporter gene (luciferase), as described above. To determine the optimal concentration of actinomycin D in our experimental system, a range of concentrations of actinomycin D (0.1–10 μg/ml) were studied. Twenty-four hours after transfection, the transcription inhibitor actinomycin D was added into the cell culture, and then the reporter gene (luciferase) mRNA level was determined by real-time PCR at different time points as described in each experiment. The cells were harvested at several time points, i.e., 0, 0.5, 1, 2, 5, 10 h after treatment with the actinomycin D inhibitor, and total RNA of the cells was extracted. Total RNA at the 0-h time point denotes cells when actinomycin D was added, i.e., 24 h after transfection with plasmid DNA. Luciferase mRNA from the 0-h time point was compared with that in samples obtained at different time points following actinomycin D addition. To compare mRNA stability among hSP-A 5′-UTR constructs, H441 cells were transfected with recombinant hSP-A 5′-UTR constructs, and gene expression was inhibited using the optimal concentration of actinomycin D (5 μg/ml of the culture medium). The cells were sampled at several time points, 0, 0.5, 1, 2, 5, 10 h after the inhibitor actinomycin D was added, and mRNA levels of the transfected gene (SP-A 5′-UTR/LUC) were determined by quantitative real-time PCR.

Statistical analysis. In the present study, at least three independent experiments were carried out. In addition, triplicate assays were performed in some experiments of reporter luciferase activity (n = 3–9). The data were analyzed by with the standard program software SigmaStat version 2.0 (SPSS). Differences between/among groups were assessed by the ANOVA test or multiple-comparison ANOVA (Tukey test). The results are expressed as means ± SE. Statistical significant differences were considered when the $P < 0.05$.

RESULTS

Generation of the constructs with hSP-A 5′-UTR sequence variants. SP-A 5′-UTR variants used in the present study were obtained from SP-A cDNA clones by PCR and were cloned into the rpcDNA3/LUC vector (Fig. 2), as described in MATERIALS AND METHODS. The four constructs under study each included one of the following hSP-A 5′-UTR splice variants, A′D′, AB′D′, A′CD′, and ABD (Fig. 1). A′D′, AB′D′, and A′CD′ variants have been previously identified as transcripts of hSP-A1 and the ABD as hSP-A2 transcript (36). The sequence alignment of the four hSP-A 5′-UTR variants is shown in Table 2.

hSP-A 5′-UTR mediates expression of reporter luciferase gene activity: a time course. First, we determined optimal conditions for the luciferase activity assay. Each of the hSP-A 5′-UTR constructs (ABD and A′CD′) along with the transfection efficiency control vector (pRL-SV40) were cotransfected into H441 cells. The transfection efficiency control vector contains the *Renilla* luciferase gene, and the *Renilla* luciferase activity serves as a denominator in our assays. The cells were harvested 36 h after transfection. Cell extracts were prepared and diluted from 0 to 100,000 times. Then, the firefly and *Renilla* luciferase activities were analyzed using the Dual-luciferase kit. The ratios of firefly-*Renilla* luciferase activity at different dilutions are shown in Table 3. The results indicated that the ratio of firefly-*Renilla* luciferase activity of cell extracts is relatively stable at a dilution range of 0–1,000 times (boldface in Table 3). In subsequent experiments we used undiluted cell extracts.

To determine the optimal time point of the luciferase activity we carried out time-course experiments with the ABD variant. The ABD construct was cotransfected into H441 cells along with the transfection efficiency control pRL-SV40 vector, and the cells were harvested after transfection at 12, 24, 30, 36, 42, and 48 h. The results indicated that the firefly luciferase activity increases from 12 to 24 h after transfection, reaching a plateau at about the 24-h time point (Fig. 3*A*). After that, no significant difference of the firefly luciferase activity was observed up to 48 h following transfection. A time course for the A′D′ construct was also performed (data not shown), and although a plateau was reached by the 36-h time point, the slope of the increase seemed different from that of the ABD

Table 2. *Sequence comparison of SP-A 5′-UTR splicing variants*

```
                10                  20                  30
A       A′
(nt 1)  (nt 6)
↓       ↓
-----GGAGGCAGAGACCCAAGCAGCTGGA                          A′D′
AACTTGGAGGCAGAGACCCAAGCAGCTGGA                          ABD
AACTTGGAGGCAGAGACCCAAGCAGCTGGA                          AB′D′
-----GGAGGCAGAGACCCAAGCAGCTGGA                          A′CD′
                40                  50                  60
                        B, B′, or C
                        (nt 45)
                        ↓
GGCCCTGTGTGTGG----------------                          A′D′
GGCTCTGTGTGTGGGTCGCTGATTTCTTGG                          ABD
GGCTCTGTGTGTGGGTCGCTGATTTCTTGG                          AB′D′
GGCTCTGTGTGTGGCCTGGAGACCCCACAA                          A′CD′
                70                  80                  90
------------------------------                          A′D′
AGCCTGAAAAGAAG----------------                          ABD
AGCCTGAAAAGAAGGTAACTGGGCATATGA                          AB′D′
CCTCCAGCCGGAGGCCTGAAGCATGAGGCC                          A′CD′
                100                 110                 120
                                        D   D′
                                    (nt 115) (nt 118)
                                        ↓   ↓
----------------------------GAG                        A′D′
--------------------------CAGGAG                        ABD
GGGACAGATGGAGTGAGTCAGTGA----GAG                         AB′D′
ATGCCAGGTGCCAG--------------GAG                         A′CD′
                130
CAGCGACTGGACCCAGAGCC                                    A′D′
CAGCGACTGGACCCAGAGCC                                    ABD
CAGCGACTGGACCCAGAGCC                                    AB′D′
CAGCGACTGGACCCAGAGCC                                    A′CD′
```

Nucleotide sequences of 5′-untranslated region (UTR) variant with underline (_____) represent exon A, with underline (_____) represent exon A′, with underline (_____) represent exon B, with underline (.....) represent exon B′, with underline (_ _ _ _) represent exon C, with underline (~~~~~) represent exon D, with underline (.....) represent exon D′. The nucleotide (nt) where each exon starts is noted (e.g. exons B, B′, or C start at nt 45).

construct. A time course of luciferase activity from 12 to 27 h after transfection indicated that the firefly luciferase activity continued to increase throughout this period, as shown in the inset of Fig. 3*A*. In subsequent experimentation, a time point in the plateau (36 h) was chosen for luciferase activity measurement so that we could more accurately compare differences among hSP-A 5′-UTR constructs.

Comparison of luciferase relative activity among hSP-A 5′-UTR splice variants. To compare 5′-UTR-mediated gene expression by each of the four hSP-A splice variants, each construct was cotransfected into H441 cells along with the pRL-SV40 vector. A construct without the hSP-A 5′-UTR variant sequence containing the SV40 promoter and the firefly luciferase gene served as an SP-A control (depicted as LUC in the figures). The cells were harvested 36 h after transfection, the luciferase activities (firefly, *Renilla*) were analyzed by the Dual-luciferase assay, and the ratio of firefly/*Renilla* luciferase activity for each construct was determined. The results (Fig. 3*B*) show that *1*) all four hSP-A 5′-UTR splice variants (ABD, A′D′, AB′D′, and A′CD′) exhibit significantly higher luciferase activity compared with the SP-A control, LUC (no hSP-A 5′-UTR) ($P < 0.01$). The level of luciferase activity increased from 2.5-fold (A′D′) to 19.5-fold (ABD) of the LUC control; *2*) the activity of the ABD splice variant is significantly higher than that of the other three variants (A′D′, AB′D′, or A′CD′) ($P < 0.01$), and the ABD activity is 7.9-fold higher than A′D′; *3*) the luciferase activity of the AB′D′ variant is significantly higher than that of A′D′ or A′CD′ ($P < 0.01$).

Role of hSP-A1 and hSP-A2 5′-UTR splice variants on mRNA levels. The luciferase activities measured above were taken to represent protein level. To further explore molecular mechanisms of the hSP-A 5′-UTR-regulated gene expression, we studied the impact of SP-A1 and SP-A2 5′-UTR on mRNA levels using quantitative real-time PCR. We performed a time-course experiment, by determining the mRNA level of luciferase of two 5′-UTR splice variants, ABD (SP-A2) and A′D′ (SP-A1) at different time points (6, 15, 18, 24, 36, 48 h) after transfection. The results shown in Fig. 4*A* indicate that the mRNA level of the ABD variant increased up to 36 h after transfection and then showed a decrease as assessed by the 48-h time point measurement. A similar pattern was observed for the A′D′-mediated mRNA level, except that the absolute level of A′D′ mRNA was lower than that of ABD.

Comparison of luciferase mRNA content among SP-A 5′-UTR splice variants. We compared hSP-A 5′-UTR-mediated luciferase mRNA level among the four 5′-UTR variants. Each of the four hSP-A 5′-UTR constructs (A′D′, ABD, AB′D′, or A′CD′) and the control (LUC) were cotransfected into H441 cells along with the pRL-SV40 control vector. Total RNA from the cells was isolated at 30 h following transfection, and the copy number of luciferase mRNA per 100 ng of total RNA was determined by quantitative real-time PCR (see MATERIALS AND METHODS). The relative luciferase mRNA content was determined following normalization of each SP-A 5′-UTR variant to LUC control. The results (Fig. 4*B*) indicated that *1*) all hSP-A 5′-UTR variants have significantly higher ($P < 0.01$) mRNA levels compared with LUC control (no hSP-A 5′-UTR). The mRNA amount of the 5′-UTR variants varies from

Table 3. *Ratio of activity of luciferase of cell extract after serial dilution*

	ABD			A′CD′		
Dilution (times)	Firefly	*Renilla*	Ratio of Firefly/*Renilla*	Firefly	*Renilla*	Ratio of Firefly/*Renilla*
Undiluted	7606735	2929531	**2.5966**	3912810	6241268	**0.6269**
10	987820	395834	**2.4956**	465398	796485	**0.5844**
100	111691	46027	**2.4243**	48933	85687	**0.5710**
1000	13028	5847	**2.2283**	5532	10104	**0.5408**
10000	1560	1305	1.1946	719	1865	0.3856
100000	689	932	0.7394	192	892	0.2158

4.3-fold (A′D′) to 8.8-fold (ABD) of the control (LUC); *2*) the ABD mRNA level is significantly higher ($P < 0.01$) compared with that of the other three constructs (A′D′, AB′D′, or A′CD′); and *3*) no significant differences are observed among AB′D′, A′D′, or A′CD′.

Translation efficiency index of hSP-A 5′-UTR variants. Comparison of the findings, shown in Fig. 3*B* (luciferase activity, which is taken to reflect protein levels) and in Fig. 4*B* (mRNA levels), indicate that although no significant differences of the mRNA content were observed among A′D′, AB′D′, and A′CD′ (Fig. 4*B*), the luciferase activity of AB′D′ was significantly higher than that of A′D′ and A′CD′ (Fig. 3*B*). The translation efficiencies of the SP-A 5′-UTR variants were evaluated using the index of luciferase activity/relative mRNA content (Fig. 5). The larger the index, the higher the translation efficiency. The results indicate that both ABD and AB′D′ showed higher translation efficiency than the control (LUC), but the translational efficiencies of A′D′ and A′CD′ were lower than that of the control (LUC). This observation indicates that the ABD and AB′D′ variants exhibit increased translational efficiencies, and the A′D′ and A′CD′ show decreased translational efficiencies, although all four 5′-UTR variants enhanced the reporter gene luciferase activity and mRNA content compared with the control vector (LUC). These results demonstrate that the hSP-A 5′-UTR plays a role in the protein translation process and that alteration of translation efficiency may be one mechanism via which the hSP-A 5′-UTR variants regulate gene expression.

Comparison of predicted hSP-A 5′-UTR mRNA secondary structures. As a prelude to gain insight into potential factors contributing to differences observed among hSP-A 5′-UTR variants, we investigated the secondary structures of hSP-A 5′-UTR (ABD, A′D′, AB′D′, and A′CD′) using algorithms to identify the most energetically favored structure for each variant. The structure of each hSP-A 5′-UTR variant alone was predicted by Zuker algorithm of the mRNA fold online program (version 3.1) (78–80). The results showed that the ABD variant forms the most stable structure compared with the other 5′-UTRs. The secondary structure of the ABD, A′D′, and AB′D′ variants is shown in Fig. 6. Based on the principle of the lowest free energy and other relevant parameters of mRNA folding, the black-paired nucleotides in the predicted structure represent the highest stability. The next optimal folding is shown sequentially by colors red, purple, blue, green, light green, and yellow. The ABD secondary structure consists of a long stable stem shown by the black-paired nucleotides and a double hairpin-like head at each end of the stable stem (Fig. 6*A*). However, the A′D, AB′D′, and A′CD′ variants (data of the A′CD′ not shown) appear to lack such a level of structural stability.

Each of the four 5′-UTR variants (when one considers only the 5′-UTR region, without including the luciferase gene and

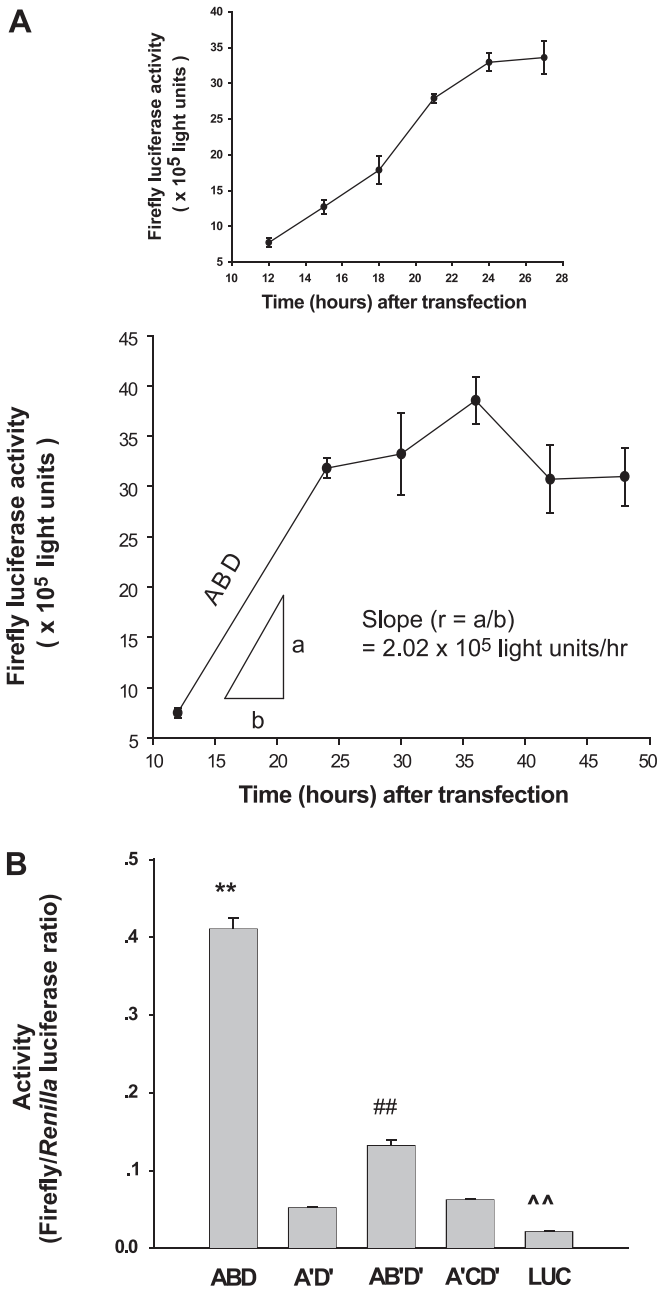

Fig. 3. hSP-A 5′-UTR mediates expression of reporter luciferase gene activity. *A*: a time course. After transient transfection of the ABD variant into H441 cells, activity measurements at various time points (12, 24, 36, 42, 48 h) were determined. The firefly luciferase activity exhibited a significant increase from 12 to ~24 h and then reached a plateau, which was maintained up to at least 50 h after transfection. The 36-h mid-time point in the plateau was used for further experimentation. The experiments were repeated 3 times ($n = 3$). Each point shows the mean ± SE. *Inset*: luciferase activity of a time course, focusing on a range from 12 to 27 h after transfection. The results indicate that the firefly luciferase activity kept increasing at this period of 12–24 h. The slope (r) of the ABD was calculated with a formula (r = a/b) (a = the increase in the amount of firefly luciferase activity from 12 to 24 h after transfection; b = the number of h from 12 to 24 h after transfection). *B*: luciferase activity. Recombinant constructs with ABD, A′D′, AB′D, A′CD′, or control vector (LUC) without hSP-A 5′-UTR variant, were cotransfected into H441 cells along with the transfection efficiency vector control (pRL-SV40). The cells were harvested 36 h after transfection, and the firefly and *Renilla* luciferase activities were measured using the Dual-luciferase assay, as described in MATERIALS AND METHODS. The ratio of firefly/*Renilla* luciferase activities was used to represent 5′-UTR-mediated gene expression. The ABD activity was significantly higher (**$P < 0.01$) than either of the constructs tested, A′D′, AB′D′, A′CD′, or control (LUC). The AB′D′ was significantly higher (##$P < 0.01$) than either A′D′, A′CD′, or control (LUC). The level of luciferase activity of the SP-A control (LUC) i.e., the rpcDNA3 construct that lacked hSP-A 5′-UTR sequence, was significantly lower (^^$P < 0.01$) than any of the constructs with hSP-A 5′-UTR variants. The experiments were repeated 3 times ($n = 3$). Bar shows ± SE.

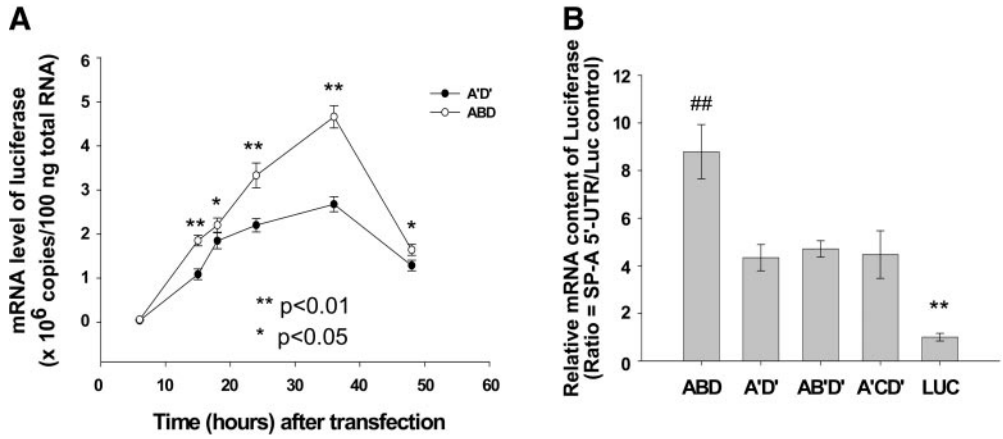

Fig. 4. hSP-A 5′UTR mediates expression of reporter luciferase gene in mRNA level. *A*: a time course. Constructs (A′D′ or ABD) along with the transfection efficiently control vector were transfected into H441 cells. The cells were harvested at different time points (6, 15, 18, 24, 36, 48 h) after transfection. Total RNAs were prepared as described in MATERIALS AND METHODS. The mRNA copies of the reporter luciferase were determined by real-time PCR. The mRNA level of each time point is shown as mRNA copy number in 100 ng of total RNA. Although the mRNA level of the ABD variant appeared to reach higher levels than A′D′ throughout the time course, their overall time-course patterns were similar. The mRNA level of luciferase exhibited a rapid increase from 6 to 36 h after transfection, and then this was followed by a decline. The experiments were repeated 3 times ($n = 3$). Each time point shows the mean ± SE. $^{**}P < 0.01$ or $^{*}P < 0.05$: significance between the A′D′ and the ABD. *B*: relative luciferase mRNA level of 4 constructs: H441 cells were transfected with each of the 4 5′-UTR constructs (ABD, A′D′, AB′D′, A′CD′) and the control (LUC) vector. RNA was prepared from the transiently transfected cells at the 30-h time point, and the mRNA levels of luciferase were determined by real-time PCR, as described in MATERIALS AND METHODS. The relative mRNA level of each SP-A 5′-UTR variant was determined following normalization of each SP-A 5′-UTR variant to LUC control. $^{**}P < 0.01$: significance between the control vector pcDNA3/LUC and each of 4 5′-UTR constructs, ABD, A′D′, AB′D′, A′CD′. $^{\#\#}P < 0.01$: significance between the ABD construct and each of the other 3 5′-UTR constructs. No significant differences at the mRNA level are detectable among A′D′, AB′D′, and A′CD′. The experiments were repeated 3 times. Bars show mean ± SE.

the 3′-UTR) has a different free energy; for the ABD variant the free energy is −35.8 kcal/mol (ABD = 100 nt, −0.358 kcal·mol^{-1}·nt^{-1}); for A′D′ it is −13.91 kcal/mol (A′D′ = 62 nt, −0.224 kcal·mol^{-1}·nt^{-1}); for AB′D′ it is −39.7 kcal/mol (AB′D′ = 137 nt, −0.289 kcal·mol^{-1}·nt^{-1}); and for A′CD′ it is −40.7 kcal/mol (A′CD′ = 122 nt, −0.334 kcal·mol^{-1}·nt^{-1}). These theoretical calculations show that the ABD variant has the lowest free energy per nt, i.e., −0.358 kcal·mol^{-1}·nt^{-1} compared with the other four 5′-UTR variants. The lower the free energy, the more stable the mRNA structure (of a given size sequence) is considered to be, compared with a similar size sequence with higher free energy.

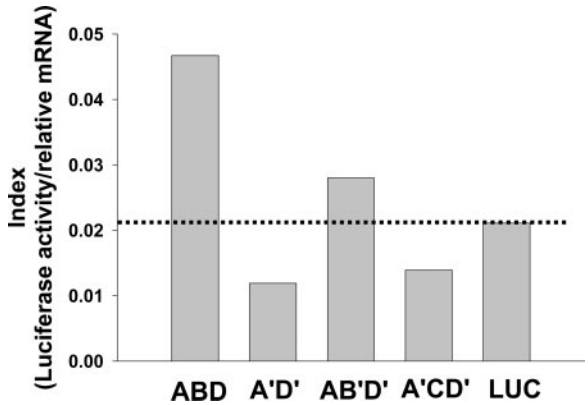

Fig. 5. hSP-A comparison of 5′-UTR-mediated translational indexes among various splice variants. The index in this figure represents the ratio of luciferase activity (firefly/*Renilla*) from Fig. 3*B* divided by the relative mRNA level of luciferase shown in Fig. 4*B*. The dotted line indicates the level of translation efficiency of control (LUC) vector (without hSP-A 5′-UTR). The indexes of ABD and AB′D′ are higher than that of control (LUC), and the indexes of constructs A′D′ and A′CD′ are lower than control.

Comparison of luciferase mRNA stability among hSP-A 5′-UTR variants. To study whether hSP-A 5′-UTR variants influence mRNA stability and whether differences in mRNA stability are observed by different hSP-A 5′-UTR variants, we evaluated the rate of mRNA decay. The luciferase mRNA level was determined by quantitative real-time PCR assays following inhibition of the RNA transcription activity by actinomycin D.

To determine the optimal concentration of the transcription inhibitor actinomycin D, a dose-response experiment was carried out using a range of concentrations (0, 0.1, 1, 5, 10 μg/ml). The H441 cells were transiently transfected with the ABD construct, and 24 h after transfection the cells were treated with actinomycin D at the indicated concentrations. The cells were harvested at several time points, 0, 0.5, 1, 2, 5, and 10 h after actinomycin D treatment. The relative mRNA levels of luciferase are shown in Fig. 7*A*. The results show that gene transcription could not be inhibited completely when the cells were treated with 0.1 or 1 μg/ml of actinomycin D (Fig. 7*A*). However, the mRNA levels decreased significantly after treatment with 5 or 10 μg/ml of actinomycin D, with no significant difference detected between 5 and 10 μg/ml of actinomycin D. Therefore, a concentration of 5 μg of actinomycin D per ml was deemed optimal and was used in subsequent experimentation.

Next, the rate of mRNA decay was compared between each of the four hSP-A 5′-UTR constructs (ABD, A′D′, AB′D′, and A′CD′) and the control (LUC) vector (without hSP-A 5′-UTR), and among the hSP-A 5′-UTR variants. These constructs were transfected into H441 cells as described in MATERIALS AND METHODS. Twenty-four hours after transfection, transcription was inhibited with actinomycin D (5 μg/ml), and the levels of luciferase mRNA transcripts at 0.5, 1, 2, 5, and 10 h

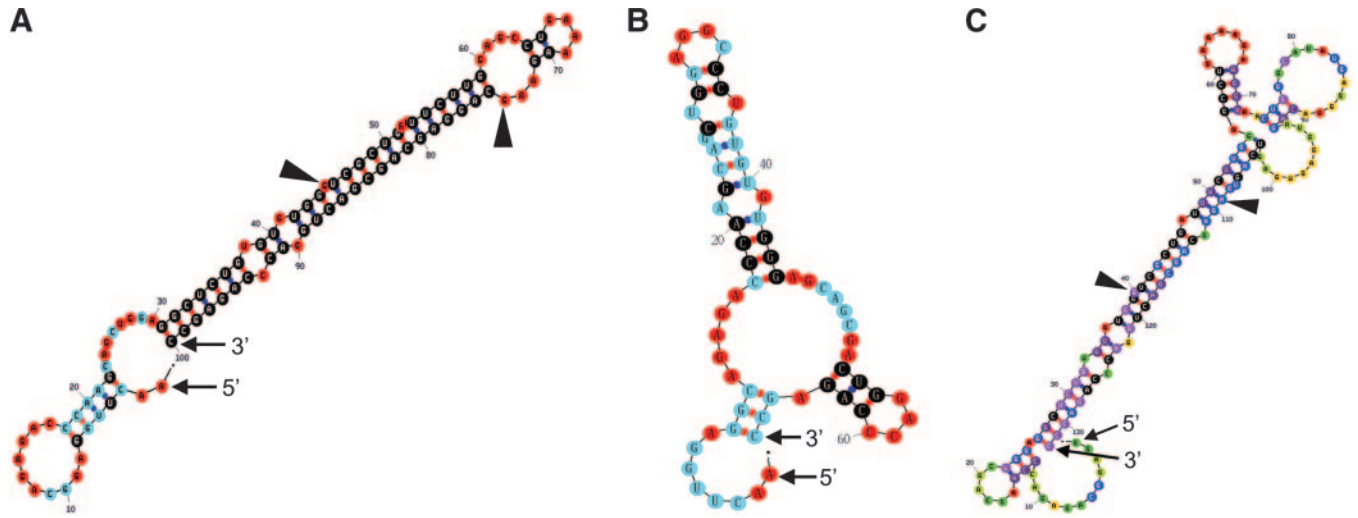

Fig. 6. Predicted secondary structures of 5′-UTR variants. The secondary structures of hSP-A 5′-UTR variants (ABD, A′D′, and AB′D′) were predicted using the Zuker algorithm (78–80) of the mRNA folding online program (version 3.1) http://www.bioinfo.rpi.edu/applications/mfold/old/rna/. The secondary structures of 5′-UTR variants are shown: ABD (*A*), A′D′ (*B*), and AB′D′ (*C*). Numbers indicate nucleotide positions in 5′-UTR; each dot represents 1 nt, and the color of the dot indicates the presumed stability of the bond in each base pair. Optimal folding is shown sequentially by colors black, red, purple, blue, green, light green, and yellow, with black and yellow representing the most and least optimal folding, respectively. In addition, the start and end nucleotides of the exon B of ABD (*A*) and the exon B′ of AB′D′ (*C*) are indicated by solid triangles.

were determined by real-time PCR. The results shown in Fig. 7*B* indicate that *1*) after treatment with the inhibitor, all four 5′-UTR variants have higher mRNA levels compared with actinomycin D-treated control (LUC) vector; *2*) the relative mRNA level of ABD is significantly higher than that of the other variants (A′D′, AB′D′, and A′CD′); and *3*) no significant differences of the rate of mRNA decay were observed among A′D′, AB′D′, and A′CD′. These observations indicate that the hSP-A 5′-UTR variants increase mRNA stability compared with the control (LUC) and that the mRNA decay is differentially affected by the 5′-UTR splice variants.

DISCUSSION

Regulation of gene expression is achieved through a series of complex mechanisms including control of processes involved in gene transcription, posttranscriptional modifications, and translation. The hSP-A locus consists of two functional genes, SP-A1 and SP-A2, and a pseudogene. SP-A1 and SP-A2 gene expression is regulated at several different levels, including developmental, tissue/cell-specific gene expression, allele-specific expression (13, 46, 52). Several regions of the hSP-A gene, including 5′-flanking and promoter regions (29) as well as the 3′-UTR (27, 72), are involved in these regulatory processes. Although the coding sequences of both SP-A1 and SP-A2 genes share a high degree of similarity, structural and functional differences between the two gene products and even among the alleles have been observed in recent studies (17, 31, 65, 71, 73, 74). Both SP-A1 and SP-A2 genes are expressed in the lung tissue and generate at least three and two 5′-UTR splice variants, respectively (36). However, it is not clear what role(s) the hSP-A 5′-UTR variants play in the regulation of SP-A expression and whether the 5′-UTR variants differentially affect SP-A expression. In the present study, we studied the role of hSP-A 5′-UTR variants in gene expression, by evaluating the role of 5′-UTR on protein, mRNA content, and mRNA stability. Our findings indicate that the 5′-UTR splice variants exhibit differential impact on several regulatory steps. The SP-A2 ABD 5′-UTR splice variant was found with higher activity, higher mRNA stability, and higher translation efficiency compared with SP-A1 variants. Of the SP-A1 variants the AB′D′ showed higher translation efficiency index, and based on theoretical considerations, a higher secondary structure stability was observed compared with A′D′ and A′CD′ variants; the mRNA stability of all three SP-A1 variants was virtually identical. We speculate that the hSP-A 5′-UTR modulates expression via several mechanisms and that 5′-UTR-mediated differences contribute to differences observed in SP-A levels among individuals.

Published work has indicated an important role for 5′-UTR in posttranscriptional modification and/or translation (19, 68). Initiation of translation is one of the most important steps that could influence the level of gene expression, and 5′-UTR sequences may greatly contribute to this step. Five structural elements near the 5′-end of the mRNA determine initiation of translational efficiency (19, 68). These are *1*) the m7G cap, *2*) the primary sequence or context surrounding the AUG codon, *3*) the presence of the AUG codons in the 5′-UTR, *4*) the secondary structure of mRNA, and *5*) the 5′-UT leader length. It is likely that the composition and/or the length of the leader sequence plays an important role in the translation efficiency and may account for differences among hSP-A 5′-UTR splice variants. Between the most frequently observed SP-A2 (ABD and ABD′) (ABD′ was not studied in this work) and SP-A1 (A′D′) variants, the length of the SP-A2 leader sequence is clearly longer (ABD and ABD′ are 100 and 97 nt, respectively) than the SP-A1 (A′D′ is 62 nt). Although the SP-A2 ABD variant with the longer leader sequence (compared with A′D′) exhibited higher translation efficiency and higher mRNA stability, other less frequently found variants with even longer leader sequence (AB′D′ = 137 nt, A′CD′ = 122 nt) than either A′D′ or ABD exhibited translation efficiency (A′CD′) equivalent to A′D′ or lower (AB′D′) than the ABD. These

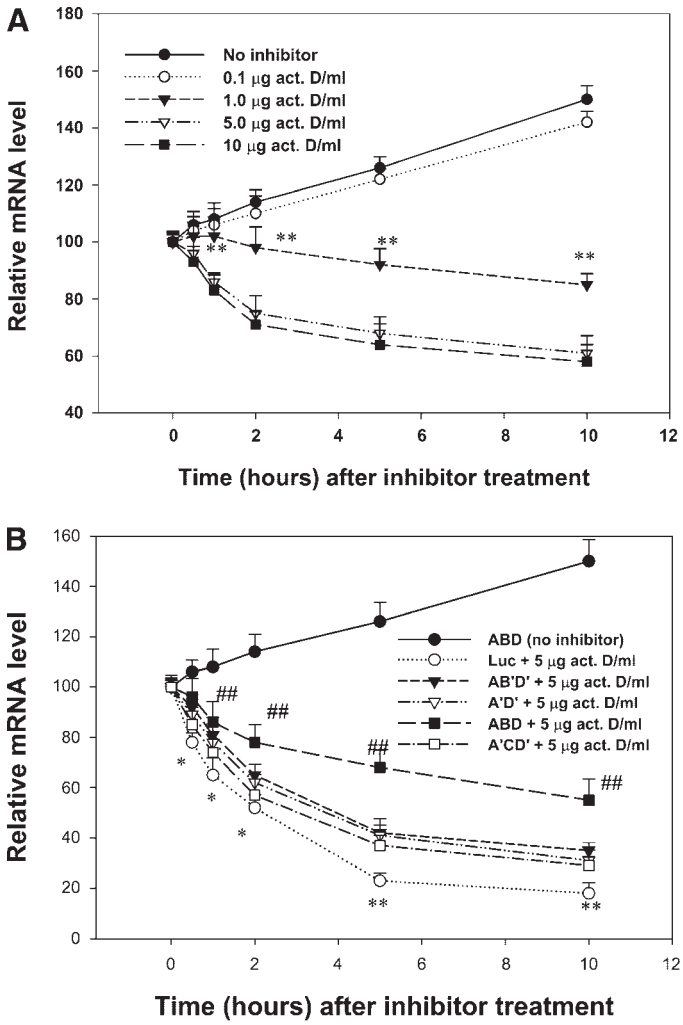

Fig. 7. Effect of 5′-UTR-mediated mRNA stability. *A*: dose-response inhibition of transcription by actinomycin D (act. D). H441 cells were transfected with the ABD construct. The cells (24 h after transfection) were treated with the transcription inhibitor act. D at various concentrations (0, 0.1, 1, 5, 10 μg/ml) and harvested at various time points (0, 0.5, 1, 2, 5, and 10 h) after treatment with the inhibitor. The luciferase mRNA level was determined by real-time PCR. The relative mRNA levels of luciferase (mRNA amount at the 0-h time point is shown as 100%) are shown. Concentrations of 0.1 μg/ml of act. D did not inhibit transcription, but concentrations of 1 μg of act. D/ml could significantly decrease transcription compared with control without act. D treatment (**$P < 0.01$). When a concentration of 5 or 10 μg of act. D/ml was used the transcriptional activity of luciferase was completely inhibited. The experiments were repeated 3 times ($n = 3$). Each point shows the mean + SE. *B*: comparison of luciferase mRNA stability among hSP-A 5′-UTR variants. H441 cells were transfected with each of the constructs, ABD, A′D′, AB′D′, A′CD′, and the control (LUC) vector. The cells were treated with the transcription inhibitor act. D (5 μg/ml) 24 h after transfection, and harvested, at time points 0, 0.5, 1, 2, 5, and 10 h after inhibitor treatment. RNA was extracted at each time point, and the amount of luciferase mRNA was measured by real-time PCR. The relative mRNA levels of luciferase are shown. The mRNA content is set to 100% at the time point of 0 h (before inhibitor treatment). All 4 5′-UTR variants exhibited higher relative mRNA levels compared with act. D-treated control (LUC) vector without hSP-A 5′-UTR (*$P < 0.05$, **$P < 0.01$). Of the 4 5′-UTR variants, the ABD variant had significantly higher relative mRNA level than the other constructs (A′D′, AB′D′, or A′CD′) (##$P < 0.01$). No significant differences were observed among A′D′, AB′D′, and A′CD′. The experiments were repeated 3 times ($n = 3$). Each point shows the mean + SE.

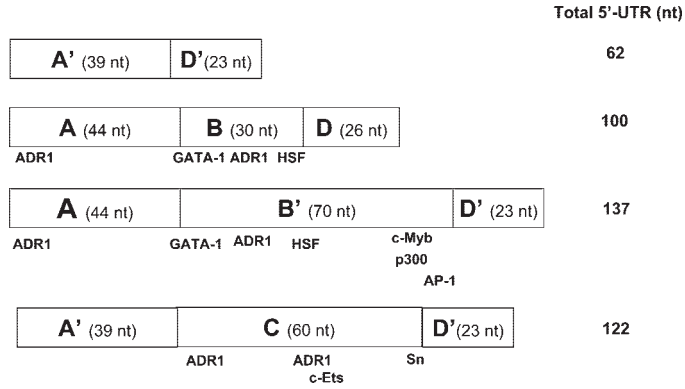

Fig. 8. Potential recognition binding sites for regulatory factors located at hSP-A 5′-UTR variants. Each exon or region of each hSP-A 5′-UTR variant is denoted with a rectangle box, and the number of base pairs of each is shown within the box. The total base pairs of each 5′-UTR variant are listed on the right. Several DNA binding factors are shown under the box for each 5′-UTR variant, where potential recognition binding sites for these factors were detected, i.e., ADR1, alcohol dehydrogenase gene regulator 1; GATA-1, GATA-binding factor 1; HSF, heat shock transcription factor; p300, a major E1A-associated cellular protein 300-kDa product; AP-1, activator protein 1; c-Myb, a hematopoietic lineage-restricted transcription factor; Sn, Snail factor.

observations support the notion that the leader sequence composition is more important than simply the length of this sequence. We speculate that the sequence composition of exon B contributes to the enhanced activity of the ABD variant, via binding of positive regulatory factors to exon B recognition binding sites. We further speculate that exon B lacks binding factors that negatively affect the translation efficiency as it may be in the case of the AB′D′ variant (see below). This putative differential regulation of translation efficiency among 5′-UTR variants may help explain the varying mRNA (14, 35) and protein (24) levels of SP-A observed among individuals. However, future experiments are warranted to determine elements that may bind to exon B and the impact of these on translation.

Cis-acting elements in 5′-UTR have been implicated in the regulation of gene expression of a number of genes. For instance, the 5′-UTR of GLUT1 glucose transporter increased the expression of the luciferase gene, and deletion of 5′- and 5′-/3′-UTRs markedly reduced the expression of luciferase, suggesting that *cis*-acting elements of 5′-UTR play important roles in the translation of GLUT1 (2–4). The effect of regulation may involve different mechanisms, such RNA-protein interactions. A well-known *cis*-acting element is iron-responsive element (IRE) (23). IRE had been identified and characterized in several genes, in which cytoplasmic RNA binding proteins, iron regulatory protein-1 (IRP-1) and IRP-2, specifically bind the mRNA stem-loop structure of IRE in the 5′-UTR and regulate translation (23, 40).

In addition, a number of DNA binding sites of regulatory factors were identified on the SP-A 5′-UTR splice variants in the present study (Fig. 8). For example, the ABD variant and specifically exon B contains recognition sites for alcohol dehydrogenase gene regulator 1, GATA-1, and heat shock transcription factor. These sites, although present in the AB′D′ variant, which showed significantly lower activity than the ABD in all the assays performed in the study, the AB′D′ variant and specifically the 3′-end of exon B′ had additional binding sites for c-Myb, p300, and activator protein (AP)-1. Currently, it is also unknown whether the regulatory binding

recognition sites present in B, B′, or C exon are functionally active, either in transcriptional regulation or other mechanism.

Our previous study has implicated an AP-1-like binding sequence within intron 1 (or between exons A and B of human SP-A) (28) in the regulation of SP-A in response to phorbol ester (28, 53). Whether the AP-1 site in exon B′ plays a role in SP-A regulation remains to be determined. It is also of interest to note that GATA-6, a member of the zinc finger protein family, has been shown to be required for maturation of the lung in late gestation (47). One study showed that transforming growth factor-β1 inhibits vascular endothelial growth factor receptor-2 gene expression and this inhibition was mediated by a palindromic GATA site located in the 5′-UTR (54). The levels of gene expression and translation efficiency have been shown to be differentially regulated through the 5′-UTR splice variants in the proinsulin gene (66), estrogen receptor-α gene (41), and heat shock protein 70 gene (62). Therefore, the potential recognition binding sites in exons B, B′, and C may contribute to changes in SP-A content via a variety of mechanisms.

The 5′-UTR has also been shown to affect translation efficiency through cap-independent internal ribosome entry site (IRES)-mediated mechanism (for reviews see Refs. 22, 67). Although this novel mechanism of the translation initiation was first discovered in picornaviral RNAs (33, 55), growing evidence indicates that some eukaryotic mRNAs also possess a similar mechanism (reviewed in Refs. 22, 67). The IRES-mediated translation initiation requires specific sequences that can form a Y-shaped secondary structure and a short stem loop near the start of the AUG codon (42, 62). About 6.4% of the human 5′-UTR sequences contain IRES, and these leader sequences are usually >200 bp in length (7, 44, 56). However, it is currently unknown whether shorter leader sequences (with <200 bp), such as the hSP-A 5′-UTR variants under study, can involve IRES-mediated translational mechanism.

Several studies have suggested that the 5′-UTR regulates gene expression by altering mRNA stability in both prokaryotic and eukaryotic cells (1, 21, 30, 77). Hambraeus et al. (21) found that a 5′-UTR stem-loop and ribosome binding are important for the stability of *Bacillus subtilis aprE* mRNA; the rate of mRNA decay of the mutated 5′-UTR of *aprE* was significantly increased compared with that of the wild-type sequence. Recently, a similar mechanism was found in eukaryotic cells (1, 30, 77). A stem-loop region of the tobacco *psbA* 5′-UTR was shown to play an important role in determining mRNA stability and translation efficiency (77), and the first 92 bp of the *At-P5R* 5′-UTR of *Arabidopsis* were sufficient in mediating mRNA stability and translation inhibition (30). These published findings indicate that 5′-UTR sequences and relevant secondary structures of transcripts from both prokaryotic and eukaryotic cells could influence both mRNA stability and/or translation efficiency. In the present study, we found that the hSP-A 5′-UTR variants appear to also modulate mRNA stability, following inhibition of transcription by actinomycin D. All four hSP-A 5′-UTR exhibited higher mRNA stability compared with the control vector (LUC), with the ABD variant showing a considerably lower rate of mRNA decay compared with the other three constructs. The present data identify differential mRNA stability as yet another mechanism of SP-A regulation. It is possible that the stability of 5′-UTR ABD secondary structure (compared to other variants) is key to higher mRNA stability observed for the ABD variant. Whether this contributes to the differential regulation of SP-A1 and SP-A2 mRNA in basal levels, in response to various agents, or during fetal lung development (32, 34, 43, 51) remains to be determined.

In summary, the hSP-A 5′-UTR variants regulate SP-A gene expression, at least through mechanisms involving mRNA stability and translation efficiency. *1*) All four hSP-A 5′-UTR variants have higher mRNA level and luciferase activity compared with the control vector without hSP-A 5′-UTR. *2*) Differences in the rate of mRNA decay and translation efficiency are observed among four 5′-UTR variants. *3*) The ABD variant has not only a lower rate of mRNA decay and possibly the most stable mRNA secondary structure, but also the highest translation efficiency among the four 5′-UTR variants studied. *4*) The AB′D′ variant has higher translation efficiency than A′D′ and A′CD′, but all three have the same rate of mRNA decay stability. *5*) Although the A′D′ and A′CD′ had a higher mRNA content and exhibited a lower rate of mRNA decay compared with the control vector, their translation efficiency indexes were lower than that of the control vector. These findings indicate that the 5′-UTR in hSP-A plays an important regulatory role in SP-A expression by modulating several levels of regulatory control.

ACKNOWLEDGMENTS

We thank Dan Krissinger and Terry Rager at the Core Facility of the Pennsylvania State University College of Medicine for assistance in the quantitative real-time PCR experiments of this project.

GRANTS

This work is supported by National Heart, Lung, and Blood Institute Grant R37 HL-34788.

REFERENCES

1. **Anderson MB, Folta K, Warpeha KM, Gibbons J, Gao J, and Kaufman LS.** Blue light-directed destabilization of the pea Lhcb1*4 transcript depends on sequences within the 5′ untranslated region. *Plant Cell* 11: 1579–1590, 1999.
2. **Boado RJ and Pardridge WM.** The 5′-untranslated region of GLUT1 glucose transporter mRNA causes differential regulation of the translational rate in plant and animal systems. *Comp Biochem Physiol B Biochem Mol Biol* 118: 309–312, 1997.
3. **Boado RJ and Pardridge WM.** Amplification of gene expression using both 5′- and 3′-untranslated regions of GLUT1 glucose transporter mRNA. *Brain Res Mol Brain Res* 63: 371–374, 1999.
4. **Boado RJ, Tsukamoto H, and Pardridge WM.** Evidence for translational control elements within the 5′-untranslated region of GLUT1 glucose transporter mRNA. *J Neurochem* 67: 1335–1343, 1996.
5. **Boggaram V, Smith ME, and Mendelson CR.** Posttranscriptional regulation of surfactant protein-A messenger RNA in human fetal lung in vitro by glucocorticoids. *Mol Endocrinol* 5: 414–423, 1991.
6. **Cannons AC and Cannon J.** The stability of the Chlorella nitrate reductase mRNA is determined by the secondary structure of the 5′-UTR: implications for posttranscriptional regulation of nitrate reductase. *Planta* 214: 488–491, 2002.
7. **Chappell SA, Edelman GM, and Mauro VP.** A 9-nt segment of a cellular mRNA can function as an internal ribosome entry site (IRES) and when present in linked multiple copies greatly enhances IRES activity. *Proc Natl Acad Sci USA* 97: 1536–1541, 2000.
8. **Crouch E and Wright JR.** Surfactant proteins A and D and pulmonary host defense. *Annu Rev Physiol* 63: 521–554, 2001.
9. **De la Cruz BJ, Prieto S, and Scheffler IE.** The role of the 5′ untranslated region (UTR) in glucose-dependent mRNA decay. *Yeast* 19: 887–902, 2002.
10. **DiAngelo S, Lin Z, Wang G, Phillips S, Ramet M, Luo J, and Floros J.** Novel, non-radioactive, simple and multiplex PCR-cRFLP methods for

genotyping human SP-A and SP-D marker alleles. *Dis Markers* 15: 269–281, 1999.

11. **Floros J and Hoover RR.** Genetics of the hydrophilic surfactant proteins A and D. *Biochim Biophys Acta* 1408: 312–322, 1998.
12. **Floros J and Phelps DS.** Pulmonary surfactant. In: *Anesthesia: Biologic Foundations*, edited by Yaksh TL, Lynch C III, Zapol WM, Maze M, Biebuck J, and Saidman LJ: Philadelphia, PA: Lippincott-Raven, 1997, p. 1259–1279.
13. **Floros J and Phelps DS.** Pulmonary surfactant protein A; structure, expression, and its role in innate host defense. In: *Surfactant-Update of Intensive Care Medicine*, edited by Nakos G and Lekka ME. Ioannina, Greece: University of Ioannina, 2002, p. 87–102.
14. **Floros J, Phelps DS, deMello DE, Longmate J, Harding H, Benson B, and White T.** The utility of postmortem lung for RNA studies; variability and correlation of the expression of surfactant proteins in human lung. *Exp Lung Res* 17: 91–104, 1991.
15. **Floros J, Steinbrink R, Jacobs K, Phelps D, Kriz R, Recny M, Sultzman L, Jones S, Taeusch HW, Frank HA, and Fritsch EF.** Isolation and characterization of cDNA clones for the 35-kDa pulmonary surfactant-associated protein. *J Biol Chem* 261: 9029–9033, 1986.
16. **Foyt HL, LeRoith D, and Roberts CT Jr.** Differential association of insulin-like growth factor I mRNA variants with polysomes in vivo. *J Biol Chem* 266: 7300–7305, 1991.
17. **Garcia-Verdugo I, Wang G, Floros J, and Casals C.** Structural analysis and lipid-binding properties of recombinant human surfactant protein a derived from one or both genes. *Biochemistry* 41: 14041–14053, 2002.
18. **Goss KL, Kumar AR, and Snyder JM.** SP-A2 gene expression in human fetal lung airways. *Am J Respir Cell Mol Biol* 19: 613–621, 1998.
19. **Gray NK and Wickens M.** Control of translation initiation in animals. *Annu Rev Cell Dev Biol* 14: 399–458, 1998.
20. **Haagsman HP, Hawgood S, Sargeant T, Buckley D, White RT, Drickamer K, and Benson BJ.** The major lung surfactant protein, SP 28–36, is a calcium-dependent, carbohydrate-binding protein. *J Biol Chem* 262: 13877–13880, 1987.
21. **Hambraeus G, Karhumaa K, and Rutberg B.** A 5′ stem-loop and ribosome binding but not translation are important for the stability of Bacillus subtilis aprE leader mRNA. *Microbiology* 148: 1795–1803, 2002.
22. **Hellen CU and Sarnow P.** Internal ribosome entry sites in eukaryotic mRNA molecules. *Genes Dev* 15: 1593–1612, 2001.
23. **Hentze MW and Kuhn LC.** Molecular control of vertebrate iron metabolism: mRNA-based regulatory circuits operated by iron, nitric oxide, and oxidative stress. *Proc Natl Acad Sci USA* 93: 8175–8182, 1996.
24. **Honda Y, Takahashi H, Shijubo N, Kuroki Y, and Akino T.** Surfactant protein-A concentration in bronchoalveolar lavage fluids of patients with pulmonary alveolar proteinosis. *Chest* 103: 496–499, 1993.
25. **Hoover DS, Wingett DG, Zhang J, Reeves R, and Magnuson NS.** Pim-1 protein expression is regulated by its 5′-untranslated region and translation initiation factor eIF-4E. *Cell Growth Differ* 8: 1371–1380, 1997.
26. **Hoover RR and Floros J.** Organization of the human SP-A and SP-D loci at 10q22-q23. Physical and radiation hybrid mapping reveal gene order and orientation. *Am J Respir Cell Mol Biol* 18: 353–362, 1998.
27. **Hoover RR and Floros J.** SP-A 3′-UTR is involved in the glucocorticoid inhibition of human SP-A gene expression. *Am J Physiol Lung Cell Mol Physiol* 276: L917–L924, 1999.
28. **Hoover RR, Pavlovic J, and Floros J.** Induction of AP-1 binding to intron 1 of SP-A1 and SP-A2 is implicated in the phorbol ester inhibition of human SP-A promoter activity. *Exp Lung Res* 26: 303–317, 2000.
29. **Hoover RR, Thomas KH, and Floros J.** Glucocorticoid inhibition of human SP-A1 promoter activity in NCI-H441 cells. *Biochem J* 340: 69–76, 1999.
30. **Hua XJ, Van de Cotte B, Van Montagu M, and Verbruggen N.** The 5′ untranslated region of the At-P5R gene is involved in both transcriptional and post-transcriptional regulation. *Plant J* 26: 157–169, 2001.
31. **Huang W, Wang G, Phelps DS, Al-Mondhiry H, and Floros J.** Human SP-A genetic variants and bleomycin-induced cytokine production by THP-1 cells: effect of ozone-induced SP-A oxidation. *Am J Physiol Lung Cell Mol Physiol* 286: L546–L553, 2004.
32. **Iannuzzi DM, Ertsey R, and Ballard PL.** Biphasic glucocorticoid regulation of pulmonary SP-A: characterization of inhibitory process. *Am J Physiol Lung Cell Mol Physiol* 264: L236–L244, 1993.
33. **Jang SK, Krausslich HG, Nicklin MJ, Duke GM, Palmenberg AC, and Wimmer E.** A segment of the 5′ nontranslated region of encephalomyocarditis virus RNA directs internal entry of ribosomes during in vitro translation. *J Virol* 62: 2636–2643, 1988.
34. **Karinch AM, Deiter G, Ballard PL, and Floros J.** Regulation of expression of human SP-A1 and SP-A2 genes in fetal lung explant culture. *Biochim Biophys Acta* 1398: 192–202, 1998.
35. **Karinch AM, deMello DE, and Floros J.** Effect of genotype on the levels of surfactant protein A mRNA and on the SP-A2 splice variants in adult humans. *Biochem J* 321: 39–47, 1997.
36. **Karinch AM and Floros J.** 5′ splicing and allelic variants of the human pulmonary surfactant protein A genes. *Am J Respir Cell Mol Biol* 12: 77–88, 1995.
37. **Karinch AM and Floros J.** Translation in vivo of 5′ untranslated-region splice variants of human surfactant protein-A. *Biochem J* 307: 327–330, 1995.
38. **Katyal SL, Singh G, and Locker J.** Characterization of a second human pulmonary surfactant-associated protein SP-A gene. *Am J Respir Cell Mol Biol* 6: 446–452., 1992.
39. **Kebaara B, Nazarenus T, Taylor R, Forch A, and Atkin AL.** The Upf-dependent decay of wild-type PPR1 mRNA depends on its 5′-UTR and first 92 ORF nucleotides. *Nucleic Acids Res* 31: 3157–3165, 2003.
40. **Kohler SA, Henderson BR, and Kuhn LC.** Succinate dehydrogenase b mRNA of Drosophila melanogaster has a functional iron-responsive element in its 5′-untranslated region. *J Biol Chem* 270: 30781–30786, 1995.
41. **Kos M, Denger S, Reid G, and Gannon F.** Upstream open reading frames regulate the translation of the multiple mRNA variants of the estrogen receptor alpha. *J Biol Chem* 277: 37131–37138, 2002.
42. **Kullmann M, Gopfert U, Siewe B, and Hengst L.** ELAV/Hu proteins inhibit p27 translation via an IRES element in the p27 5′UTR. *Genes Dev* 16: 3087–3099, 2002.
43. **Kumar AR and Snyder JM.** Differential regulation of SP-A1 and SP-A2 genes by cAMP, glucocorticoids, and insulin. *Am J Physiol Lung Cell Mol Physiol* 274: L177–L185, 1998.
44. **Le SY and Maizel JV Jr.** A common RNA structural motif involved in the internal initiation of translation of cellular mRNAs. *Nucleic Acids Res* 25: 362–369, 1997.
45. **Lin Z, deMello D, Phelps DS, Koltun WA, Page M, and Floros J.** Both human SP-A1 and Sp-A2 genes are expressed in small and large intestine. *Pediatr Pathol Mol Med* 20: 367–386, 2001.
46. **Lin Z and Floros J.** Heterogeneous allele expression of pulmonary SP-D gene in rat large intestine and other tissues. *Physiol Genomics* 11: 235–243, 2002.
47. **Liu C, Morrisey EE, and Whitsett JA.** GATA-6 is required for maturation of the lung in late gestation. *Am J Physiol Lung Cell Mol Physiol* 283: L468–L475, 2002.
48. **MacNeill C, Umstead TM, Phelps DS, Lin Z, Floros J, Shearer DA, and Weisz J.** Surfactant protein A, an innate immune factor, is expressed in the vaginal mucosa and is present in vaginal lavage fluid. *Immunology* 111: 91–99, 2004.
49. **Madsen J, Tornoe I, Nielsen O, Koch C, Steinhilber W, and Holmskov U.** Expression and localization of lung surfactant protein A in human tissues. *Am J Respir Cell Mol Biol* 29: 591–597, 2003.
50. **McCormack FX and Whitsett JA.** The pulmonary collectins, SP-A and SP-D, orchestrate innate immunity in the lung. *J Clin Invest* 109: 707–712, 2002.
51. **McCormick SM and Mendelson CR.** Human SP-A1 and SP-A2 genes are differentially regulated during development and by cAMP and glucocorticoids. *Am J Physiol Lung Cell Mol Physiol* 266: L367–L374, 1994.
52. **Mendelson CR.** Role of transcription factors in fetal lung development and surfactant protein gene expression. *Annu Rev Physiol* 62: 875–915, 2000.
53. **Miakotina OL and Snyder JM.** Signal transduction events involved in TPA downregulation of SP-A gene expression. *Am J Physiol Lung Cell Mol Physiol* 286: L1210–L1219, 2004.
54. **Minami T, Rosenberg RD, and Aird WC.** Transforming growth factor-beta 1-mediated inhibition of the flk-1/KDR gene is mediated by a 5′-untranslated region palindromic GATA site. *J Biol Chem* 276: 5395–5402, 2001.
55. **Pelletier J and Sonenberg N.** Internal initiation of translation of eukaryotic mRNA directed by a sequence derived from poliovirus RNA. *Nature* 334: 320–325, 1988.
56. **Pesole G, Mignone F, Gissi C, Grillo G, Licciulli F, and Liuni S.** Structural and functional features of eukaryotic mRNA untranslated regions. *Gene* 276: 73–81, 2001.

57. **Phelps DS.** Surfactant regulation of host defense function in the lung: a question of balance. *Pediatr Pathol Mol Med* 20: 269–292, 2001.
58. **Phelps DS and Floros J.** Localization of pulmonary surfactant proteins using immunohistochemistry and tissue in situ hybridization. *Exp Lung Res* 17: 985–995, 1991.
59. **Phelps DS and Floros J.** Localization of surfactant protein synthesis in human lung by in situ hybridization. *Am Rev Respir Dis* 137: 939–942, 1988.
60. **Phelps DS, Taeusch HW Jr, Benson B, and Hawgood S.** An electrophoretic and immunochemical characterization of human surfactant-associated proteins. *Biochim Biophys Acta* 791: 226–238, 1984.
61. **Rogers JT, Randall JD, Cahill CM, Eder PS, Huang X, Gunshin H, Leiter L, McPhee J, Sarang SS, Utsuki T, Greig NH, Lahiri DK, Tanzi RE, Bush AI, Giordano T, and Gullans SR.** An iron-responsive element type II in the 5′-untranslated region of the Alzheimer's amyloid precursor protein transcript. *J Biol Chem* 277: 45518–45528, 2002.
62. **Rubtsova MP, Sizova DV, Dmitriev SE, Ivanov DS, Prassolov VS, and Shatsky IN.** Distinctive properties of the 5′-untranslated region of human hsp70 mRNA. *J Biol Chem* 278: 22350–22356, 2003.
63. **Saitoh H, Okayama H, Shimura S, Fushimi T, Masuda T, and Shirato K.** Surfactant protein A2 gene expression by human airway submucosal gland cells. *Am J Respir Cell Mol Biol* 19: 202–209, 1998.
64. **Scavo LM, Ertsey R, and Gao BQ.** Human surfactant proteins A1 and A2 are differentially regulated during development and by soluble factors. *Am J Physiol Lung Cell Mol Physiol* 275: L653–L669, 1998.
65. **Selman M, Lin HM, Montano M, Jenkins AL, Estrada A, Lin Z, Wang G, DiAngelo SL, Guo X, Umstead TM, Lang CM, Pardo A, Phelps DS, and Floros J.** Surfactant protein A and B genetic variants predispose to idiopathic pulmonary fibrosis. *Hum Genet* 113: 542–550, 2003.
66. **Shalev A, Blair PJ, Hoffmann SC, Hirshberg B, Peculis BA, and Harlan DM.** A proinsulin gene splice variant with increased translation efficiency is expressed in human pancreatic islets. *Endocrinology* 143: 2541–2547, 2002.
67. **Vagner S, Galy B, and Pyronnet S.** Irresistible IRES. Attracting the translation machinery to internal ribosome entry sites. *EMBO Rep* 2: 893–898, 2001.
68. **Van der Velden AW and Thomas AA.** The role of the 5′ untranslated region of an mRNA in translation regulation during development. *Int J Biochem Cell Biol* 31: 87–106, 1999.
69. **Voss T, Melchers K, Scheirle G, and Schafer KP.** Structural comparison of recombinant pulmonary surfactant protein SP-A derived from two human coding sequences: implications for the chain composition of natural human SP-A. *Am J Respir Cell Mol Biol* 4: 88–94, 1991.
70. **Wadkins RM, Vladu B, and Tung CS.** Actinomycin D binds to metastable hairpins in single-stranded DNA. *Biochemistry* 37: 11915–11923, 1998.
71. **Wang G, Bates-Kenney SR, Tao JQ, Phelps DS, and Floros J.** Differences in biochemical properties and in biological function between human SP-A1 and SP-A2 variants, and the impact of ozone-induced oxidation. *Biochemistry* 43: 4227–4239, 2004.
72. **Wang G, Guo X, and Floros J.** Human SP-A 3′-UTR variants mediate differential gene expression in basal levels and in response to dexamethasone. *Am J Physiol Lung Cell Mol Physiol* 284: L738–L748, 2003.
73. **Wang G, Phelps DS, Umstead TM, and Floros J.** Human SP-A protein variants derived from one or both genes stimulate TNF-alpha production in the THP-1 cell line. *Am J Physiol Lung Cell Mol Physiol* 278: L946–L954, 2000.
74. **Wang G, Umstead TM, Phelps DS, Al-Mondhiry H, and Floros J.** The effect of ozone exposure on the ability of human surfactant protein a variants to stimulate cytokine production. *Environ Health Perspect* 110: 79–84, 2002.
75. **West CA, Arnett TR, and Farrow SM.** Expression of insulin-like growth factor I (IGF-I) mRNA variants in rat bone. *Bone* 19: 41–46, 1996.
76. **White RT, Damm D, Miller J, Spratt K, Schilling J, Hawgood S, Benson B, and Cordell B.** Isolation and characterization of the human pulmonary surfactant apoprotein gene. *Nature* 317: 361–363, 1985.
77. **Zou Z, Eibl C, and Koop HU.** The stem-loop region of the tobacco psbA 5′UTR is an important determinant of mRNA stability and translation efficiency. *Mol Genet Genomics* 269: 340–349, 2003.
78. **Zuker M.** Calculating nucleic acid secondary structure. *Curr Opin Struct Biol* 10: 303–310, 2000.
79. **Zuker M.** Mfold web server for nucleic acid folding and hybridization prediction. *Nucleic Acids Res* 31: 3406–3415, 2003.
80. **Zuker M and Jacobson AB.** Using reliability information to annotate RNA secondary structures. *RNA* 4: 669–679, 1998.